Astronomy & Astrophysics

LETTER TO THE EDITOR

The Hubble constant determined through an inverse distance ladder including quasar time delays and Type Ia supernovae

S. Taubenberger[1], S. H. Suyu[1,2,3], E. Komatsu[1,4], I. Jee[1], S. Birrer[5], V. Bonvin[6], F. Courbin[6], C. E. Rusu[7,8,9], A. J. Shajib[5], and K. C. Wong[4,7]

[1] Max-Planck-Institut für Astrophysik, Karl-Schwarzschild-Str. 1, 85748 Garching, Germany
e-mail: `tauben@mpa-garching.mpg.de`
[2] Physik-Department, Technische Universität München, James-Franck-Str. 1, 85748 Garching, Germany
[3] Institute of Astronomy and Astrophysics, Academia Sinica, 11F of ASMAB, No.1, Section 4, Roosevelt Rd., Taipei 10617, Taiwan
[4] Kavli Institute for the Physics and Mathematics of the Universe (Kavli IPMU, WPI), Univ. of Tokyo, Kashiwa 277-8583, Japan
[5] Department of Physics and Astronomy, University of California, Los Angeles, CA 90095-1547, USA
[6] Laboratoire d'Astrophysique, École Polytechnique Fédérale de Lausanne (EPFL), Observatoire de Sauverny, 1290 Versoix, Switzerland
[7] National Astronomical Observatory of Japan, 2-21-1 Osawa, Mitaka, Tokyo 181-8588, Japan
[8] Subaru Telescope, National Astronomical Observatory of Japan, 650 N Aohoku Pl, Hilo 96720, Japan
[9] Department of Physics, University of California, Davis, 1 Shields Avenue, Davis, CA 95616, USA

ABSTRACT

Context. The precise determination of the present-day expansion rate of the Universe, expressed through the Hubble constant H_0, is one of the most pressing challenges in modern cosmology. Assuming flat ΛCDM, H_0 inference at high redshift using cosmic microwave background data from *Planck* disagrees at the 4.4σ level with measurements based on the local distance ladder made up of parallaxes, Cepheids, and Type Ia supernovae (SNe Ia), often referred to as Hubble tension. Independent cosmological-model-insensitive ways to infer H_0 are of critical importance.
Aims. We apply an inverse distance ladder approach, combining strong-lensing time-delay distance measurements with SN Ia data. By themselves, SNe Ia are merely good indicators of relative distance, but by anchoring them to strong gravitational lenses we can obtain an H_0 measurement that is relatively insensitive to other cosmological parameters.
Methods. A cosmological parameter estimate was performed for different cosmological background models, both for strong-lensing data alone and for the combined lensing + SNe Ia data sets.
Results. The cosmological-model dependence of strong-lensing H_0 measurements is significantly mitigated through the inverse distance ladder. In combination with SN Ia data, the inferred H_0 consistently lies around 73–74 km s^{-1} Mpc^{-1}, regardless of the assumed cosmological background model. Our results agree closely with those from the local distance ladder, but there is a $>2\sigma$ tension with *Planck* results, and a ~1.5σ discrepancy with results from an inverse distance ladder including *Planck*, baryon acoustic oscillations, and SNe Ia. Future strong-lensing distance measurements will reduce the uncertainties in H_0 from our inverse distance ladder.

Key words. gravitational lensing: strong – cosmological parameters – distance scale

1. Introduction

Ever since Georges Lemaître and Edwin Hubble discovered that our Universe is expanding (Lemaître 1927, 1931; Hubble 1929), astronomers have sought to measure the Hubble constant H_0 that characterises the present-day expansion rate. For decades there was the "factor of 2 controversy" in the H_0 measurements, culminating in the *Hubble* Space Telescope Key Project that pinned down H_0 to 72 ± 8 km s^{-1} Mpc^{-1} using the Cepheids distance ladder with several secondary distance indicators including Type Ia Supernovae (SNe Ia) (Freedman et al. 2001; Freedman 2017). In recent years, another controversy on H_0 has emerged, particularly between the measurements based on the cosmic microwave background (CMB; $H_0 = 67.36 \pm 0.54$ km s^{-1} Mpc^{-1} for flat ΛCDM; Planck Collaboration VI 2018) and the local distance ladder (SH0ES programme; $H_0 = 74.03 \pm 1.42$ km s^{-1} Mpc^{-1}; Riess et al. 2019). The value of H_0 inferred from the CMB depends on the background cosmology, and the 4.4σ tension

between the *Planck* and SH0ES measurements refers to a standard flat ΛCDM cosmology with a spatially flat Universe consisting of cold dark matter and a dark energy that is described by the cosmological constant Λ.

This tension, if not resolved by systematic effects (e.g., Rigault et al. 2015, 2018; Jones et al. 2018; Roman et al. 2018), indicates new physics beyond flat ΛCDM (e.g., Di Valentino et al. 2018; Mörtsell & Dhawan 2018; Adhikari & Huterer 2019; Agrawal et al. 2019; Kreisch et al. 2019; Pandey et al. 2019; Poulin et al. 2019; Vattis et al. 2019). Independent measurements of H_0 are particularly important in order to verify this tension, given the potential of discovering new physics. Methods based on Type IIP supernova expanding photospheres (Schmidt et al. 1994; Gall et al. 2016), water masers (Gao et al. 2016; Braatz et al. 2019), or standard sirens (Schutz 1986; The LIGO Scientific Collaboration et al. 2017) have recently provided independent H_0 measurements. While they currently have uncertainties that are consistent with both the

Planck and the SH0ES measurements, future measurements with larger samples of Type IIP supernovae, water masers, and standard sirens could reduce their uncertainties to help shed light on the H_0 tension.

Gravitationally lensed quasars are another competitive and independent cosmological probe, particularly in measuring H_0. When a quasar is strongly lensed by a foreground galaxy, multiple time-delayed images of the quasar appear around the lens. By measuring the time delays between the multiple quasar images and modelling the mass distributions of both the lens galaxy and other structures along the line of sight, strong lensing provides a measurement of the time-delay distance ($D_{\Delta t}$), which is a combination of the angular diameter distances between the observer and the lens (D_d), the observer and the quasar (D_s), and the lens and the quasar (D_{ds}): $D_{\Delta t} = (1 + z_d)D_d D_s/D_{ds}$ (Refsdal 1964; Suyu et al. 2010; Treu & Marshall 2016). While $D_{\Delta t}$ is inversely proportional and mostly (but not only) sensitive to H_0, the inference of H_0 from $D_{\Delta t}$ measurements depends on the cosmological model. In addition, stellar velocity dispersions of the foreground lens galaxies, if available, provide a determination of D_d, which can further constrain cosmological models (Paraficz & Hjorth 2009; Jee et al. 2015, 2016, 2019).

The H0LiCOW project (Suyu et al. 2017), in Collaboration with the COSMOGRAIL programme (Courbin et al. 2018), has assembled a sample of lensed quasar systems with exquisitely measured time-delay distances (Bonvin et al. 2017; Wong et al. 2017; Birrer et al. 2019). Through a blind analysis, Birrer et al. (2019) reported $H_0 = 72.5^{+2.1}_{-2.3}$ km s^{-1} Mpc^{-1} (3% uncertainty, including systematics) from the data of four lensed quasars, in flat ΛCDM. However, as in all cosmological experiments that measure distances outside the scope of the linear Hubble relation $D = cz/H_0$, the inference of H_0 from $D_{\Delta t}$ depends on the assumed background cosmology. While much focus in the community is on H_0 in flat ΛCDM, a cosmological-model-independent inference of H_0 is valuable.

The inverse distance ladder (Aubourg et al. 2015; Cuesta et al. 2015) provides a way to infer H_0 which is more model-independent. The idea is to anchor the relative distances from SNe Ia with an absolute distance measurement. Supernova distances on their own are not absolute distances because of the unknown intrinsic luminosity of SNe (e.g. Leibundgut et al. 2017). Nonetheless, SNe map out the expansion history of the Universe very precisely, and by anchoring their distance scale with absolute distance measurements, cosmological-model-insensitive absolute distance determinations become feasible. By anchoring the SN distance scale using distances measured from baryon acoustic oscillations (BAO), Macaulay et al. (2019) measured an H_0 from the Dark Energy Survey consistent with that provided by the Planck Collaboration VI (2018) and that does not depend much on cosmological models, although the inference of H_0 is strongly affected by the assumptions of the size of the sound horizon (Aylor et al. 2019). Recently, Jee et al. (2019) and Wojtak & Agnello (2019) anchored the SN distance scale using D_d measured from strongly lensed quasars, resulting in H_0 values with ~10% uncertainty, limited by the precision of the D_d measurements. With current data, lensed quasars yield tighter constraints on $D_{\Delta t}$ than D_d. In this paper, we explore the use of $D_{\Delta t}$ as anchor.

This Letter is organised as follows. In Sect. 2 we summarise the $D_{\Delta t}$ measurements from the four H0LiCOW lenses, and in Sect. 3 we use these distances to infer H_0 through the inverse distance ladder. We discuss the results in Sect. 4, and provide an outlook in Sect. 5. Throughout the paper, our parameter constraints correspond to the median values of the parameter

Table 1. Lens redshifts (z_d) and source redshifts (z_s) of the strongly lensed quasars from H0LiCOW included in this study.

Name	z_d	z_s	References
B1608+656	0.6304	1.394	1, 2
RX J1131−1231	0.295	0.654	3, 2
HE 0435−1223	0.4546	1.693	4, 2
SDSS 1206+4332	0.745	1.789	5

References. (1) Suyu et al. (2010); (2) Bonvin et al. (2017); (3) Suyu et al. (2014); (4) Wong et al. (2017); (5) Birrer et al. (2019)

probability distributions, with 68% credibility intervals given by the 16th and 84th percentiles.

2. Lensing time-delay distances

We use the posterior probability distribution of $D_{\Delta t}$, $P(D_{\Delta t})$, for the four lensed quasar systems that have been measured by the H0LiCOW Collaboration (listed in Table 1). For three systems (B1608+656, RX J1131−1231, and HE 0435−1223; Suyu et al. 2010, 2014; Sluse et al. 2017; Rusu et al. 2017; Wong et al. 2017; Tihhonova et al. 2018), $P(D_{\Delta t})$ is nicely described by the analytic fit

$$P(D_{\Delta t}) = \frac{1}{\sqrt{2\pi}(x - \lambda_D)\sigma_D} \exp\left[-\frac{(\ln(x - \lambda_D) - \mu_D)^2}{2\sigma_D^2}\right], \qquad (1)$$

where $x = D_{\Delta t}/(1\,\mathrm{Mpc})$, and the fitted parameter values (λ_D, σ_D, μ_D) are listed in Table 3 of Bonvin et al. (2017). For the fourth lens system (SDSS 1206+4332), we use the Markov chain Monte Carlo (MCMC) results for $D_{\Delta t}$ from Birrer et al. (2019)[1], and obtain $P(D_{\Delta t})$ through a kernel density estimator.

3. Inverse distance ladder: supernovae anchored with strongly lensed quasars

To determine the joint likelihood of cosmological parameters for different experiments and cosmological models, we employ the MontePython v3.1 MCMC sampling package (Audren et al. 2013; Brinckmann & Lesgourgues 2018), which is interfaced with the Boltzmann code CLASS (Lesgourgues 2011) for CMB calculations. As MCMC algorithm, we select MontePython's Metropolis-Hastings sampler. For every combination of cosmological probes and assumed cosmological background model, we start with a relatively short MCMC chain (~50 000 steps) with dynamic updates of the covariance matrix and jumping factor (known as the super-update strategy in MontePython; Brinckmann & Lesgourgues 2018), which ensures an efficient sampling and an acceptance rate close to the optimal 25%. This is followed by a fully Markovian chain of 500 000 steps, where the covariance matrix and jumping factor are kept fixed at the previously determined values. Our long chains have acceptance rates between 15% and 30% and show good convergence.

The sampling includes the H_0 and Ω_{CDM} parameters[2] and, for cosmological models other than flat ΛCDM, combinations of Ω_k, w_0, and w_a. The priors employed for these cosmological parameters are summarised in Table 2. They can have an impact

---

[1] The chain of the joint constraint on $D_{\Delta t}$ and D_d is released on the H0LiCOW website (http://www.h0licow.org), and we focus on $D_{\Delta t}$, marginalising over D_d.

[2] The baryon energy density Ω_b is fixed at 0.05, so that Ω_m and Ω_{CDM} can be used interchangeably.

Table 2. Priors on cosmological parameters (all uniform) as employed in the MontePython MCMC sampling.

Parameter	Minimum	Maximum
Ω_{CDM}	0	0.45
Ω_k	-0.2	0.2
w_0	-2.5	0.5
w_a	-2.0	2.0
H_0	0	150

on the inferred parameter posteriors, so we make sure that they are either physically motivated or sufficiently conservative. In those runs where strong-lensing data are combined with SN Ia data, four additional nuisance parameters (M_B, α, β, and Δ_M) are added. They represent the absolute B-band magnitude, the coefficients of light curve stretch (X_1) and colour (C) corrections, and the host-galaxy mass step, respectively, in a SALT2 framework (Guy et al. 2007; Mosher et al. 2014; Betoule et al. 2014):

$$\mu = m_B - (M_B - \alpha \times X_1 + \beta \times C + \Delta_M). \quad (2)$$

The (luminosity) distance modulus, $\mu = 5\log_{10}(D_L/1\,\mathrm{Mpc}) + 25$, is thereby calculated as the difference between the apparent peak magnitude in the rest frame B band (m_B), and the stretch- and colour-corrected absolute B-band magnitude. The empirical mass step-correction Δ_M is only added for SN host galaxies with stellar masses $\geq 10^{10}\,M_\odot$ (Sullivan et al. 2010).

We first concentrate on the cosmological parameter inference using H0LiCOW $D_{\Delta t}$ data of strongly lensed quasars alone. Four different background cosmologies are investigated: flat ΛCDM; flat wCDM with a redshift-independent dark energy equation-of-state parameter w, which can differ from -1 (corresponding to Λ); flat w_0w_aCDM with a redshift-dependent dark energy equation-of-state parameter $w(z) = w_0 + w_a\frac{z}{1+z}$; and non-flat ΛCDM, which covers the possibilities of a negatively or positively curved Universe. The resulting cosmological parameters are shown in Table 3. The energy densities of matter (Ω_m), a cosmological constant (Ω_Λ), or a more generic form of dark energy (Ω_{DE}) are not tightly constrained by the lensed quasars alone, but the effect of different background cosmologies is very weak for these parameters. For non-ΛCDM models, w deviates from -1 by more than 1σ, while the curvature in the non-flat ΛCDM case is consistent with zero. The Hubble constant shows a moderately strong dependence on the background cosmology, in particular on the dark energy equation of state, being 72.9 in both the flat and non-flat ΛCDM cases, but >80 in the flat wCDM and w_0w_aCDM cosmologies. This can be explained by the lensed-quasar systems spanning redshifts between ~0.3 (for the most nearby lens) and ~1.8 (for the most distant quasar; see Table 1), and the necessary extrapolation to obtain the present-day expansion rate of the Universe being cosmological-model-dependent, for example due to degeneracy between H_0 and w (Fig. 1).

The dependence of H_0 on the assumed background cosmology can be mitigated by combining the quasar $D_{\Delta t}$ measurements with SN data from the joint light curve analysis (JLA), which is a compilation of 740 spectroscopically confirmed low-z, SDSS-II, and SNLS SNe Ia (Betoule et al. 2014). In this inverse distance ladder approach, the SN Ia data are anchored near their high-z end by the lensed quasars, and allow for a much improved measurement of the present-day expansion rate compared to the quasar time delays alone. We employ the same priors on cosmological parameters as before (Table 2). In addition to the cosmological models investigated in the lenses-only case, we now also include the more flexible non-flat wCDM and non-flat

w_0w_aCDM models, which did not converge in the lenses-only MCMC chains. The results are again summarised in Table 3. The posteriors for Ω_m and Ω_Λ (or Ω_{DE}) have tightened up significantly compared to the lenses-only case, which is a merit of SNe Ia being able to map out the relative expansion history of the Universe very well. Similarly, the dark energy equation-of-state parameter w in the non-ΛCDM models is now better constrained, and very close to -1 in all models. The inferred curvature in the non-flat geometries is slightly larger than before, but still consistent with zero. The Hubble constant, finally, shows only a $\sim2\%$ variation with the assumed background cosmology, lying between 72.7 and 74.1 km s^{-1} Mpc^{-1} in all cases. The increased median and uncertainty observed for non-ΛCDM cosmologies obtained from lensed quasars alone is no longer an issue when combined with SN Ia data.

For two selected background cosmologies (flat wCDM and non-flat ΛCDM), the full posterior distributions for the sampled cosmological parameters are shown in Fig. 1. The improved constraints on H_0 and w (in flat wCDM) and on Ω_m (in non-flat ΛCDM) when including SN Ia data are evident. Figure 2 compares the marginalised 1D H_0 posteriors obtained from lensed quasars alone with those obtained from a combination of lensing and SN Ia data for different cosmological models. Using the inverse distance ladder, the peak-to-peak scatter in the median H_0 values of these four models is impressively reduced from 11% to 1%.

4. Discussion

We now investigate how our H_0 results compare to those from other cosmological probes: the SH0ES (Riess et al. 2019) and *Planck* (Planck Collaboration VI 2018) experiments, and a *Planck* + BAO + SNe Ia inverse distance ladder (Aubourg et al. 2015).

The local distance ladder underlying the SH0ES determination of H_0 is anchored to parallaxes at $z = 0$. It is therefore almost completely insensitive to the cosmological background model. As shown in Fig. 3, our inverse distance ladder measurements of H_0 for different cosmologies all agree very nicely with the SH0ES results of $H_0 = 74.03 \pm 1.42$ km s^{-1} Mpc^{-1}.

Inference of H_0 based on CMB, on the contrary, takes place at $z > 1000$, and involves extrapolation to $z = 0$ by assuming a cosmological model. Hence, while the *Planck* results for H_0 are very precise once a flat ΛCDM cosmology is assumed, they can vary widely if this assumption is dropped. The Planck Collaboration VI (2018) provides H_0 values only for flat ΛCDM ($H_0 = 67.36 \pm 0.54$ km s^{-1} Mpc^{-1}) and non-flat ΛCDM ($H_0 = 63.6^{+2.1}_{-2.3}$ km s^{-1} Mpc^{-1}) cosmologies, and already these differ significantly (see Fig. 3). With cosmologies that do not assume a cosmological constant, no meaningful constraints on H_0 can be obtained from the CMB alone. Our inverse distance ladder results show a tension of just above 2σ with *Planck* for both flat ΛCDM and non-flat ΛCDM, which is lower than the tension between *Planck* and SH0ES owing to our larger error bars compared to SH0ES.
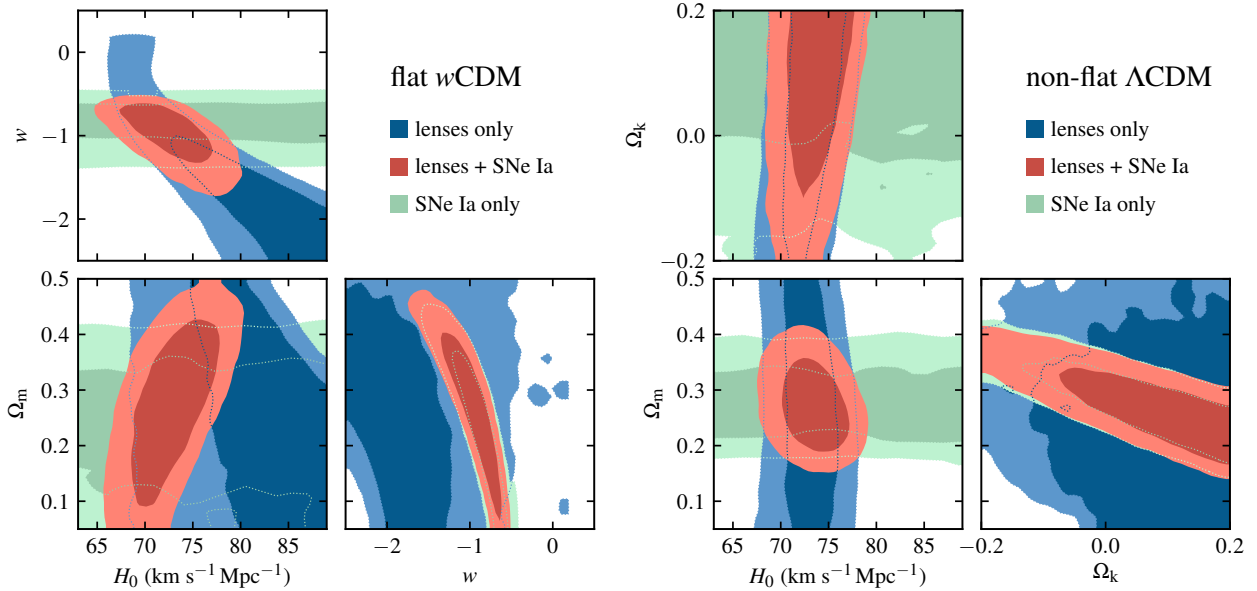
Finally, the *Planck* + BAO + SNe Ia inverse distance ladder of Aubourg et al. (2015) is anchored to BAO absolute distances at redshifts 0.1–0.6. CMB data are used to set the sound-horizon scale, which BAO distances are inversely proportional to. The inferred values of H_0 for different cosmological models are in good agreement with each other, clustering between 67 and 68 km s^{-1} Mpc^{-1}, with uncertainties between 1.0% and 1.5%. The discrepancy with our lensing-based inverse distance ladder is between 1.3 and 1.9σ, which is not huge, but systematic. A possible origin of this discrepancy could be the adopted sound-horizon scale from *Planck*, which is the only early-Universe property that enters into the Aubourg et al. (2015) measurement.

Table 3. Cosmological parameters extracted with MontePython MCMC sampling.

Cosmological model	Ω_m	Ω_{CDM}	Ω_Λ	Ω_{DE}	Ω_k	w_0	w_a	H_0
Lenses only								
Flat ΛCDM	$0.26^{+0.15}_{-0.14}$	$0.21^{+0.15}_{-0.14}$	$0.74^{+0.14}_{-0.15}$	$\equiv 0$	$\equiv 0$	$\equiv -1$	$\equiv 0$	$72.9^{+2.1}_{-2.3}$
Flat wCDM	$0.26^{+0.14}_{-0.14}$	$0.21^{+0.14}_{-0.14}$	$\equiv 0$	$0.74^{+0.14}_{-0.14}$	$\equiv 0$	$-1.74^{+0.60}_{-0.45}$	$\equiv 0$	$80.8^{+5.3}_{-7.1}$
Flat w_0w_aCDM	$0.27^{+0.14}_{-0.14}$	$0.22^{+0.14}_{-0.14}$	$\equiv 0$	$0.73^{+0.14}_{-0.14}$	$\equiv 0$	$-1.76^{+0.54}_{-0.44}$	$-0.26^{+1.37}_{-1.21}$	$81.2^{+5.1}_{-6.3}$
Non-flat ΛCDM	$0.26^{+0.15}_{-0.14}$	$0.21^{+0.15}_{-0.14}$	$0.72^{+0.16}_{-0.18}$	$\equiv 0$	$0.03^{+0.12}_{-0.15}$	$\equiv -1$	$\equiv 0$	$72.9^{+2.3}_{-2.4}$
Lenses + SNe Ia								
Flat ΛCDM	$0.30^{+0.04}_{-0.03}$	$0.25^{+0.04}_{-0.03}$	$0.70^{+0.03}_{-0.04}$	$\equiv 0$	$\equiv 0$	$\equiv -1$	$\equiv 0$	$73.1^{+2.1}_{-2.2}$
Flat wCDM	$0.28^{+0.10}_{-0.11}$	$0.23^{+0.10}_{-0.10}$	$\equiv 0$	$0.72^{+0.11}_{-0.10}$	$\equiv 0$	$-0.96^{+0.21}_{-0.10}$	$\equiv 0$	$72.7^{+3.0}_{-2.9}$
Flat w_0w_aCDM	$0.32^{+0.08}_{-0.11}$	$0.27^{+0.08}_{-0.11}$	$\equiv 0$	$0.68^{+0.11}_{-0.08}$	$\equiv 0$	$-0.97^{+0.20}_{-0.29}$	$-0.38^{+1.01}_{-1.08}$	$73.1^{+3.0}_{-3.0}$
Non-flat ΛCDM	$0.27^{+0.06}_{-0.05}$	$0.22^{+0.06}_{-0.05}$	$0.66^{+0.08}_{-0.06}$	$\equiv 0$	$0.08^{+0.09}_{-0.13}$	$\equiv -1$	$\equiv 0$	$73.4^{+2.2}_{-2.3}$
Non-flat wCDM	$0.27^{+0.09}_{-0.11}$	$0.22^{+0.09}_{-0.11}$	$\equiv 0$	$0.65^{+0.15}_{-0.12}$	$0.08^{+0.09}_{-0.14}$	$-1.02^{+0.24}_{-0.34}$	$\equiv 0$	$73.6^{+3.3}_{-3.3}$
Non-flat w_0w_aCDM	$0.30^{+0.08}_{-0.10}$	$0.25^{+0.08}_{-0.10}$	$\equiv 0$	$0.62^{+0.14}_{-0.11}$	$0.09^{+0.08}_{-0.14}$	$-1.05^{+0.25}_{-0.36}$	$-0.29^{+1.02}_{-1.14}$	$74.1^{+3.1}_{-3.3}$

Notes. Results for different cosmological models are shown for quasar time delays alone (upper four lines) and for the combination of the time-delay measurements with the JLA SN Ia sample (lower six lines). The quoted numbers are the median values, while the uncertainties correspond to the 16th and 84th percentiles.

Fig. 1. Contour plots with 68% and 95% confidence regions for H_0, Ω_m, and w in a flat wCDM cosmology (*left-hand side*), and for H_0, Ω_m, and Ω_k in a non-flat ΛCDM cosmology (*right-hand side*). Contours based on quasar time delays and SNe Ia (JLA compilation) alone are shown in blue and green, respectively, while those using the inverse distance ladder with both probes combined are overplotted in red.
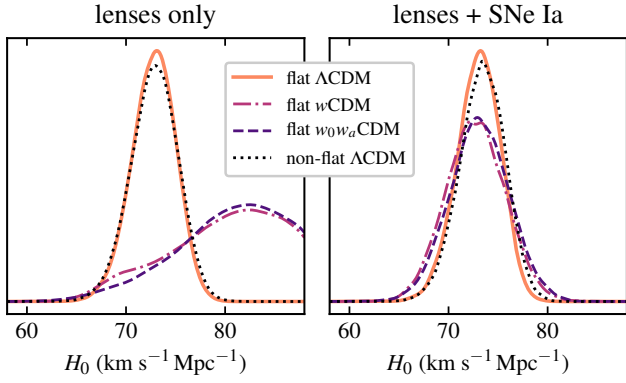
5. Outlook

On their own SNe Ia are poor probes of the absolute distance scale of the Universe (and hence H_0). In our inverse distance ladder experiment, where an anchor is provided at high redshift by time-delay distances of strongly lensed quasars, their main role is to extrapolate these absolute distance measurements back to redshift zero. This allows us to constrain H_0 in a way which is (1) rather insensitive to the assumed cosmological background model and (2) independent of Cepheids and the CMB. The Hubble constant derived from this approach (72.7–74.1 km s^{-1} Mpc^{-1}) is consistent with that obtained with the local distance ladder, but deviates at the $\sim$1.5–2σ level from results based on *Planck* CMB measurements. The origin of this discrepancy can only be speculated about, but the sound horizon determined by *Planck* certainly warrants further investigation.
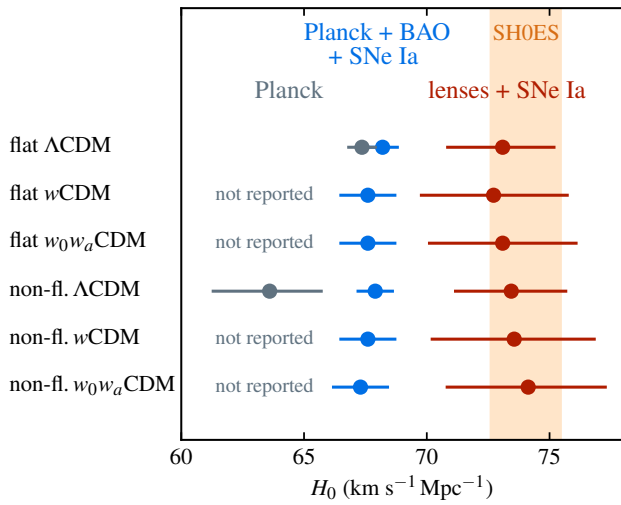
The small ($\sim$2%) dependence of H_0 on the assumed cosmological model in our inverse distance ladder implies that the precision of the H_0 inference of 3%–4% is currently limited by the

$D_{\Delta t}$ data for lensed quasars. So far the number of $D_{\Delta t}$ measurements is small: merely four strongly lensed quasars have been published by the H0LiCOW Collaboration thus far. However, more are soon to come (Rusu et al. 2019a; Chen et al. 2019), and systematic searches through various surveys[3] are yielding new lensed quasar systems. Some of these are now being monitored by the COSMOGRAIL Collaboration for time-delay measurements (Courbin et al. 2018; Millon et al. in prep.). With the upcoming Large Synoptic Survey Telescope (LSST) and Euclid surveys, many more $D_{\Delta t}$ measurements are expected, both for strongly lensed quasars and for SNe. Accordingly, the statistical

---

[3] These surveys include the Dark Energy Survey (DES) (particularly STRIDES; Treu et al. 2018), *Gaia*, the Hyper-Suprime Cam (HSC) survey, the Kilo-Degree Survey (KiDS), the Panoramic Survey Telescope and Rapid Response System (Pan-STARRS) and the Asteroid Terrestrial-impact Last Alert System (VST-ATLAS) (e.g., Agnello et al. 2018; Krone-Martins et al. 2018; Lemon et al. 2018; Spiniello et al. 2018; Rusu et al. 2019b).

Fig. 2. H_0 posteriors for different cosmologies using H0LiCOW time-delay distance measurements of four strongly lensed quasars only (*left*), and using the combination of the lensing measurements with the JLA SN Ia data set (*right*).

Fig. 3. Comparison between the quasar time-delay + SNe Ia inverse distance ladder with other cosmological probes: CMB data from *Planck* (Planck Collaboration VI 2018; TT,TE,EE + lowE + lensing), a *Planck* + BAO + SNe Ia inverse distance ladder from Aubourg et al. (2015), and Cepheid + SN Ia data from the SH0ES project (Riess et al. 2019). The mean and 68% confidence intervals for H_0 for different background cosmologies are shown for *Planck* and the two inverse distance ladders. The orange-shaded region reflects the 68% confidence interval for the SH0ES distance ladder, which is anchored locally and is thus insensitive to the cosmological background model.

uncertainty on H_0 from $D_{\Delta t}$ measurements will shrink substantially in the upcoming years (Shajib et al. 2018), rendering the inverse distance ladder approach that couples time-delay distances with SN Ia data one of the most promising methods for solving the current Hubble-tension puzzle.

References

Adhikari, S., & Huterer, D. 2019, ArXiv e-prints [arXiv:1905.02278]
Agnello, A., Schechter, P. L., Morgan, N. D., et al. 2018, MNRAS, 475, 2086
Agrawal, P., Cyr-Racine, F. Y., Pinner, D., & Randall, L. 2019, ArXiv e-prints [arXiv:1904.01016]
Aubourg, É., Bailey, S., Bautista, J. E., et al. 2015, Phys. Rev. D, 92, 123516
Audren, B., Lesgourgues, J., Benabed, K., & Prunet, S. 2013, JCAP, 2, 001
Aylor, K., Joy, M., Knox, L., et al. 2019, ApJ, 874, 4
Betoule, M., Kessler, R., Guy, J., et al. 2014, A&A, 568, A22
Birrer, S., Treu, T., Rusu, C. E., et al. 2019, MNRAS, 484, 4726
Bonvin, V., Courbin, F., Suyu, S. H., et al. 2017, MNRAS, 465, 4914
Braatz, J., Pesce, D., Condon, J., & Reid, M. 2019, in Science with a Next-Generation VLA, ed. E. J. Murphy (San Francisco, CA: ASP), ASP Monogaph Ser. in press
Brinckmann, T., & Lesgourgues, J. 2018, ArXiv e-prints [arXiv:1804.07261]
Chen, G. C.-F., Fassnacht, C. D., Suyu, S. H., et al. 2019, MNRAS, submitted [arXiv:1907.02533]
Courbin, F., Bonvin, V., Buckley-Geer, E., et al. 2018, A&A, 609, A71
Cuesta, A. J., Verde, L., Riess, A., & Jimenez, R. 2015, MNRAS, 448, 3463
Di Valentino, E., Linder, E. V., & Melchiorri, A. 2018, Phys. Rev. D, 97, 043528
Freedman, W. L. 2017, Nat. Astron., 1, 0121
Freedman, W. L., Madore, B. F., Gibson, B. K., et al. 2001, ApJ, 553, 47
Gall, E. E. E., Kotak, R., Leibundgut, B., et al. 2016, A&A, 592, A129
Gao, F., Braatz, J. A., Reid, M. J., et al. 2016, ApJ, 817, 128
Guy, J., Astier, P., Baumont, S., et al. 2007, A&A, 466, 11
Hubble, E. 1929, Proc. Natl. Acad. Sci., 15, 168
Jee, I., Komatsu, E., & Suyu, S. H. 2015, JCAP, 2015, 033
Jee, I., Komatsu, E., Suyu, S. H., & Huterer, D. 2016, JCAP, 4, 031
Jee, I., Suyu, S. H., Komatsu, E., et al. 2019, Science, in press
Jones, D. O., Riess, A. G., Scolnic, D. M., et al. 2018, ApJ, 867, 108
Kreisch, C. D., Cyr-Racine, F. Y., & Doré, O. 2019, ArXiv e-prints [arXiv:1902.00534]
Krone-Martins, A., Delchambre, L., Wertz, O., et al. 2018, A&A, 616, L11
Leibundgut, B. 2017, in History of Supernovae as Distance Indicators, eds. A. W. Alsabti, & P. Murdin (Berlin: Springer), 2525
Lemaître, G. 1927, Annales de la Société Scientifique de Bruxelles, 47, 49
Lemaître, G. 1931, MNRAS, 91, 483
Lemon, C. A., Auger, M. W., McMahon, R. G., & Ostrovski, F. 2018, MNRAS, 479, 5060
Lesgourgues, J. 2011, ArXiv e-prints [arXiv:1104.2932]
Macaulay, E., Nichol, R. C., Bacon, D., et al. 2019, MNRAS, 486, 2184
Mörtsell, E., & Dhawan, S. 2018, JCAP, 9, 025
Mosher, J., Guy, J., Kessler, R., et al. 2014, ApJ, 793, 16
Pandey, K. L., Karwal, T., & Das, S. 2019, ArXiv e-prints [arXiv:1902.10636]
Paraficz, D., & Hjorth, J. 2009, A&A, 507, L49
Planck Collaboration VI. 2018, A&A, submitted [arXiv:1807.06209]
Poulin, V., Smith, T. L., Karwal, T., & Kamionkowski, M. 2019, Phys. Rev. Lett., 122, 221301
Refsdal, S. 1964, MNRAS, 128, 307
Riess, A. G., Casertano, S., Yuan, W., Macri, L. M., & Scolnic, D. 2019, ApJ, 876, 85
Rigault, M., Aldering, G., Kowalski, M., et al. 2015, ApJ, 802, 20
Rigault, M., Brinnel, V., Aldering, G., et al. 2018, A&A, submitted [arXiv:1806.03849]
Roman, M., Hardin, D., Betoule, M., et al. 2018, A&A, 615, A68
Rusu, C. E., Fassnacht, C. D., Sluse, D., et al. 2017, MNRAS, 467, 4220
Rusu, C. E., Wong, K. C., Bonvin, V., et al. 2019a, MNRAS, submitted [arXiv:1905.09338]
Rusu, C. E., Berghea, C. T., Fassnacht, C. D., et al. 2019b, MNRAS, 486, 4987
Schmidt, B. P., Kirshner, R. P., Eastman, R. G., et al. 1994, ApJ, 432, 42
Schutz, B. F. 1986, Nature, 323, 310
Shajib, A. J., Treu, T., & Agnello, A. 2018, MNRAS, 473, 210
Sluse, D., Sonnenfeld, A., Rumbaugh, N., et al. 2017, MNRAS, 470, 4838
Spiniello, C., Agnello, A., Napolitano, N. R., et al. 2018, MNRAS, 480, 1163
Sullivan, M., Conley, A., Howell, D. A., et al. 2010, MNRAS, 406, 782
Suyu, S. H., Marshall, P. J., Auger, M. W., et al. 2010, ApJ, 711, 201
Suyu, S. H., Treu, T., Hilbert, S., et al. 2014, ApJ, 788, L35
Suyu, S. H., Bonvin, V., Courbin, F., et al. 2017, MNRAS, 468, 2590
Tihonova, O., Courbin, F., Harvey, D., et al. 2018, MNRAS, 477, 5657
The LIGO Scientific Collaboration, the Virgo Collaboration, the 1M2H Collaboration, et al. 2017, Nature, 551, 85
Treu, T., & Marshall, P. J. 2016, A&ARv, 24, 11
Treu, T., Agnello, A., Baumer, M. A., et al. 2018, MNRAS, 481, 1041
Vattis, K., Koushiappas, S. M., & Loeb, A. 2019, Phys. Rev. D, 99, 121302
Wojtak, R., & Agnello, A. 2019, MNRAS, 486, 5046
Wong, K. C., Suyu, S. H., Auger, M. W., et al. 2017, MNRAS, 465, 4895